Caffeic acid and hydroxytyrosol have anti-obesogenic properties in zebrafish and rainbow trout models

Esmail Lutfi[1], Patrick J. Babin[2]*, Joaquim Gutiérrez[1], Encarnación Capilla[1], Isabel Navarro[1]*

1 Department of Cell Biology, Physiology and Immunology, Faculty of Biology, University of Barcelona, Barcelona, Spain, **2** Maladies Rares: Génétique et Métabolisme (MRGM), University of Bordeaux, INSERM, U12211, Pessac, France

* mnavarro@ub.edu (IN); p.babin@gpp.u-bordeaux1.fr (PJB)

Abstract

Some natural products, known sources of bioactive compounds with a wide range of properties, may have therapeutic values in human health and diseases, as well as agronomic applications. The effect of three compounds of plant origin with well-known dietary antioxidant properties, astaxanthin (ATX), caffeic acid (CA) and hydroxytyrosol (HT), on zebrafish (*Danio rerio*) larval adiposity and rainbow trout (*Onchorynchus mykiss*) adipocytes was assessed. The zebrafish obesogenic test (ZOT) demonstrated the anti-obesogenic activity of CA and HT. These compounds were able to counteract the obesogenic effect produced by the peroxisome proliferator-activated receptor gamma (PPARγ) agonist, rosiglitazone (RGZ). CA and HT suppressed RGZ-increased PPARγ protein expression and lipid accumulation in primary-cultured rainbow trout adipocytes. HT also significantly reduced plasma triacylglycerol concentrations, as well as mRNA levels of the *fasn* adipogenic gene in the adipose tissue of HT-injected rainbow trout. In conclusion, *in vitro* and *in vivo* approaches demonstrated the anti-obesogenic potential of CA and HT on teleost fish models that may be relevant for studying their molecular mode of action. Further studies are required to evaluate the effect of these bioactive components as food supplements for modulating adiposity in farmed fish.

Introduction

Obesity has become a worldwide epidemic and is considered one of the most serious public health problems of our time [1,2]. Overweight and obesity occur when energy intake exceeds energy expenditure, leading to increased storage of triacylglycerols (TAG), mainly in white adipose tissue (WAT). In addition to TAG storage in adipocyte lipid droplets, WAT has been recognized as a multi-functional endocrine organ that plays a critical role in modulating several physiological processes, such as appetite, whole-body energy metabolism and homeostasis, as well as tissue inflammation responses [3]. Consequently, concomitant with enlarged fat

storage, pathological overgrowth of WAT is associated with a range of related problems, including type II diabetes, insulin resistance, hypertension and cardiovascular diseases [4].

One of the key molecules that modulates WAT activity in response to extrinsic signals is peroxisome proliferator-activated receptor gamma (PPARγ), a master regulator of adipogenesis that activates the transcription of a large number of genes involved in adipocyte differentiation and lipid accumulation [5]. Furthermore, PPARγ controls the expression of many factors secreted by WAT that influence insulin sensitivity, which in turn, modulate the expression of genes involved in glucose homeostasis [6]. Impaired PPARγ signaling, expression and/or activation are thus implicated in the prevalence of metabolic obesogenesis and weight-related diseases, such as diabetes. The most widely studied therapeutic use of PPARγ has been in the treatment of insulin resistance and type II diabetes. Synthetic ligands/agonists of PPARγ, e.g. thiazolidinediones, commonly used as insulin sensitizers for treating hyperglycemia in patients with type II diabetes, are of great clinical significance [7]. Nevertheless, despite their effectiveness in normalizing blood glucose levels, these compounds present detrimental side effects, such as weight gain, edema and cardiovascular complications [8]. Thus, the discovery or development of new compounds that modulate the PPARγ signaling pathway more effectively and safely, while promoting health benefits, is currently a matter of great interest.

Throughout history, natural products have provided a rich source of inspiration for drug discovery. Significant research has recently been undertaken to identify PPARγ modulators, with the aim of formulating a novel treatment to maximize antiobesity effects, in addition to antioxidant and protective properties [9]. Natural antioxidants modulate WAT inflammation produced by the overproduction of reactive oxygen species or pathological processes associated with obesity. While caffeic acid (CA), hydroxytyrosol (HT) and astaxanthin (ATX) are interesting examples of dietary compounds with proven antioxidant properties [10–12], their specific potential for treating obesity has not been fully recognized. Furthermore, the increasing use of plant-based aquafeeds has aroused great interest in the identification of new vegetal ingredients that may respond not only to the demand for sustainable aquaculture, but also, to help develop new diets that may reduce unwanted perivisceral WAT in farmed fish.

In basic research, mammalian models (e.g. mice and rats primarily) have been traditionally used in human physiology and disease research, due to their anatomical and physiological similarities [13]. Nevertheless, they could be unsuited for certain types of studies [14]. In the past decade, teleost species have been regarded as excellent alternative models for studying human diseases [15,16] and now constitute an emerging method for assessing bioactive compounds in food research [17]. A number of *in vitro* and *in vivo* studies have highlighted the applicability of several fish species within the areas of lipid metabolism and adipose tissue biology [18–23]. Besides its simplicity and numerous other advantages, fish research models such as zebrafish (*Danio rerio*) or rainbow trout (*Onchorynchus mykiss*), are very promising for obesity research, as most of the metabolic pathways linked to the lipid metabolism are conserved between mammals and teleost fish [24–26]. Indeed, histological studies have revealed also evolutionarily conserved morphological structures of teleost adipocytes [27–29].

In this study, three selected antioxidant dietary compounds (CA, HT, and ATX) were used *in vitro* and *in vivo*, to assess their potential anti-obesogenic effect on zebrafish and rainbow trout models.

Materials and methods

Animal care and ethics statement

Wild-type zebrafish were produced in our facilities at the University of Bordeaux in accordance with the French Directive (Ministère de l'Agriculture, de l'Agroalimentaire et de la

Forêt), under permit number A33-522-6. All experiments were conducted in conformity with the European Communities Council Directive (2010/63/EU) on the protection of animals used for scientific purposes and local French legislation on the care and use of laboratory animals. Larvae were obtained by natural mating and raised in embryo water (90 μg/ml Instant Ocean [Aquarium Systems, Sarrebourg, France], 0.58 mM $CaSO_4$, $2H_2O$, dissolved in reverse-osmosis purified water) at 28.5°C with an 11L:13D photoperiod. From 5 days postfertilization until day 15, larvae were fed *ad libitum* on ZF Biolabs formulated diet flakes (Tres Cantos, Spain). They were then nourished with standard diet (SD) for late larvae (TetraMin Baby, Tetra GmbH, Melle, Germany). Animal stages were recorded according to standard length, i.e. the distance from the rostral tip of the larva to the base of the caudal fin.

Juvenile rainbow trout, body weight approximately 80 g for *in vivo* studies and 250 g for extracting WAT to be used in adipocyte primary cultures, were obtained from the "Viveros de los Pirineos" fish farm (El Grado, Huesca, Spain). Animals were maintained according to the Ethics and Animal Care Committee of the University of Barcelona, following the regulations and procedures established by the Spanish and Catalan governments (CEEA 170/14, CEEA 311/15, DAAM 7952).

Reagents

HT (ref. 70604, CAS N°10597-60-1) and rosiglitazone (RGZ) (ref. 71740, CAS N°122320-73-4) were purchased from Cayman chemicals (Ann Arbor, MI). CA (ref. C0625, CAS N°331-39-5), sesame oil (ref. S3547), DMSO (ref. D8418), and ethyl 3-aminobenzoate methanesulfonate (MS-222) (ref. E10521) were provided by Sigma-Aldrich (Tres Cantos, Spain). Certified analytical grade ATX (ref. DRE-CA10307000, CAS N°472-61-7) was purchased from Dr. Ehrenstorfer GmbH (Augsburg, Germany). Stock solutions were stored at -20°C and working solutions were diluted in 0.1% DMSO on the day of the experiment.

Zebrafish obesogenic test (ZOT)

The short-term ZOT assay, using Nile red staining, is a non-invasive *in vivo* method for visualizing the effects of the molecules tested on the adiposity dynamics of zebrafish larvae by fluorescence microscopy. The 3-day, *in vivo*, animal treatment protocol was performed as previously described [30]. In replicated experiments, ten larvae ranging from 7 to 9 mm standard length were used per group. Larvae were exposed to the selected compounds or to vehicle alone for one day in a fasting state. All larvae were kept in a fasting state for 24 h prior to exposure and until the end of the trial, to avoid food auto-fluorescence. Treatments were as follows: vehicle control (CT) (0.1% DMSO), CA (0.1% DMSO plus 50 μM CA), HT (0.1% DMSO plus 100 μM HT), and ATX (0.1% DMSO plus 100 μM ATX). Concentrations of each molecule tested were the highest that did not induce any mortality. Quantitative analysis was performed, as previously described [30], by recording the image area of Nile red green fluorescence as a percentage of initial adiposity, using ImageJ software (National Institutes of Health, Bethesda, MD, USA).

Rainbow trout adipocyte cell cultures

All cell-culture reagents were purchased from Sigma-Aldrich (Tres Cantos, Spain) and Life Technologies (Alcobendas, Spain). All plastic items and glass cover slips were obtained from Nunc (LabClinics, Barcelona, Spain). Cells were cultured according to the previously established procedure [31], with perivisceral WAT from four to six fish per culture. After counting, cells were seeded at a final density of $2-2.5 \cdot 10^4$ cells/cm^2 in 1% gelatin on pretreated six-well plates (9.6 cm^2/well) for real-time quantitative PCR (qRT-PCR) analyses or twelve-well plates

(2.55 cm^2/well), with or without coverslips, for immunofluorescence or Oil red O (ORO) staining, respectively. Plates were kept at 18˚C in Leibovitz's L-15 growth medium, supplemented with 10% fetal bovine serum and 1% antibiotic-antimycotic solution (growth medium, GM). When necessary, the standard procedure used for cell differentiation was the following: once confluence was reached (day 7), cells were induced to differentiate by incubating them with a differentiation medium (DM) based on GM and containing 10 μg/mL insulin, 0.5 mM 3-isobutyl-1-methylxanthine and 0.25 μM dexamethasone. The medium was changed every 2 days throughout the procedure.

Immunofluorescence assay

Post-confluent pre-adipocyte cells from day 7 of culture were incubated with vehicle CT (DM ± 0.1% DMSO) or vehicle plus CA (50 μM), HT (100 μM) or RGZ (1 μM), or a combination of CA or HT with RGZ, for 24 h. RGZ was used as a potential rainbow trout peroxisome proliferator-activated receptor gamma (PPARγ) agonist. PPARγ was detected by immunofluorescence, using the protocol described by [32]. The polyclonal rabbit anti-PPARγ (H-100) was purchased from Santa Cruz Biotechnology (Santa Cruz, CA). Secondary Alexa Fluor® conjugated antibody (A21069, goat anti-rabbit 568) was purchased from Life Technologies (Alcobendas, Spain). Nuclei were counterstained with Hoechst (H1399, Life Technologies, Alcobendas, Spain). Images were obtained at 36x magnification on a Leica TCS-SP5 confocal microscope. Nucleus fluorescence was quantified and normalized to the total number of nuclei in the same field, using ImageJ software (National Institutes of Health, Bethesda, MD, USA).

Western blot analysis

Post-confluent pre-adipocyte cells from day 7 of culture were treated as described in the previous immunofluorescence section. Protein extraction and Western blot analysis were performed using the protocol described by [32]. Briefly, the amount of protein from each sample was measured [33] and 20 μg were subjected to electrophoresis (SDS-PAGE) on 10% polyacrylamide gels (125 V for 1 h 30 min). After overnight transfer to a PVDF membrane, a staining with Ponceau S solution (Sigma-Aldrich, Tres Cantos, Spain) was performed, showing similar amounts of transferred proteins on each lane and membranes were scanned for posterior band quantification. Subsequently, membranes were washed and then blocked in non-fat milk 5% and incubated with polyclonal rabbit anti-PPARγ (H-100), an antibody that has been previously shown to successfully cross-react with rainbow trout [31,34]. After washing, membranes were incubated with a peroxidase-conjugated secondary goat anti-rabbit antibody (Cat. No. 31460. Thermo Scientific, Alcobendas, Spain). The immunoreactive band was visualized using an enhanced chemiluminescence kit (Pierce ECL Western blotting Substrate; Thermo Scientific, Alcobendas, Spain) and quantified by densitometric scanning using ImageJ software (National Institutes of Health, Bethesda, MD, USA). Results from the densitometry analysis of each specific band were normalized by the densitometry values of the most abundant band of Ponceau S staining as previously reported [35]. In support of this methodology, it has been shown that reversible Ponceau S staining can be used advantageously over specific proteins detection for quality or control of equal loading in Western blotting [36,37].

Oil red O staining and lipid quantification

After confluence (day 7), cells were incubated with vehicle CT (DM ± 0.1% DMSO) or vehicle plus CA (50 μM), HT (100 μM), LIP (10 μl/ml) or the indicated combination of CA or HT with LIP, for 72 h. Cell differentiation and lipid accumulation were analyzed by ORO staining, as described elsewhere [38], with minor modifications. Briefly, cells were fixed with 10%

formalin for 1 h. Fixed cells were rinsed with PBS, stained with 0.3% ORO prepared in 36% tri-ethyl phosphate for 2 h, and then rinsed three times with distilled water. A 100% 2-propanol solution was used to elute the ORO dye and absorbance was measured at 490 nm. The cells were then stained with Coomassie blue for 1 h and proteins were extracted using 85% propylene glycol at 60°C for 1 h. Lipid quantification was calculated as the absorbance measured at 490 nm divided by the measurement corresponding to protein at 630 nm.

Cell viability assay

Pre-confluent pre-adipocyte cells (day 5 of culture) were incubated with vehicle CT (GM) or vehicle plus CA (50 μM), HT (100 μM), RGZ (1 μM), or a combination of CA or HT with RGZ, for 24 h. The methylthiazolyldiphenyl-tetrazolium bromide (MTT) assay was performed as previously described elsewhere [38]. Briefly, after 24 h incubation with a final concentration of 0.5 mg/mL MTT, cells were washed with PBS and the blue formazan crystals that formed were resuspended in 250 μL DMSO per well for 2 h. Cell viability values were obtained from the absorbance measured at 570 nm, with 680 nm as the reference wavelength, using a microplate reader (Infinite 200, Tecan).

Measuring cell proliferation

Pre-confluent pre-adipocyte cells (day 5 of culture) were incubated as described in the previous cell viability section. Cell proliferation was evaluated by immunocytochemical detection of proliferating cell nuclear antigen (PCNA), using a commercial staining kit (Cat. No. 93–1143, Life Technologies, Alcobendas, Spain). In brief, after 24 h incubation (see above), cells were washed and fixed in 4% paraformaldehyde (PFA, Sigma-Aldrich, Spain) at room temperature for 15 min. Subsequently, coverslips were post-fixed in 50% and 70% ethanol for 5 min and incubated in PCNA staining reagents, following the manufacturer's suggested protocol. The amount of PCNA-labeled nuclei (positive cells) was evaluated and normalized to the number of nuclei in that field, using ImageJ software (National Institutes of Health, Bethesda, MD, USA). Five to ten images were taken per coverslip with a CC2 camera coupled to a microscope at 40x using analySIS (Soft Imaging System) software.

In vivo experimental treatment in rainbow trout

After 15 days' acclimation in our facilities at 15°C, juvenile rainbow trout fasted for 24 h were then anesthetized with MS-222 (0.1 g/L) prior to receiving an intraperitoneal injection of 4.64 μL volume per g body weight. Treatments were as follows: vehicle CT containing DMSO diluted in sesame oil (1:3, v/v), vehicle plus CA at 10 μg/g body weight, and vehicle plus HT at 20 μg/g body weight. After 24 h exposure to the compounds in a fasting state, trout were anesthetized, sacrificed by a blow to the head, and blood samples were taken from the caudal aorta. Liver and perivisceral WAT samples were then harvested and preserved at −80°C pending analysis. None of the molecules tested induced mortality at the concentrations used.

Biochemical analysis of plasma parameters

Plasma samples were analyzed using commercial enzyme kits: glucose (Monlab, Barcelona, Spain), non-esterified fatty acids (NEFAs, Wako Chemicals GmbH, Neuss, Germany), and TAG and glycerol (Sigma-Aldrich, Tres Cantos, Spain).

RNA extraction, cDNA synthesis and qRT-PCR

Total RNAs from WAT (100 mg), liver (50 mg), and primary adipocyte cells (3 wells) were extracted using TriReagent (Ambion, Alcobendas, Spain), according to the manufacturer's recommendations. Treatments for *in vitro* studies were as follows: vehicle CT (DM ± 0.1% DMSO) or vehicle plus CA (50 μM), HT (100 μM), RGZ (1 μM), LIP (10 μl/ml) or the indicated combination of CA or HT with RGZ or LIP, for 24 h. A ND-2000 NanoDrop spectrophotometer (Thermo Fisher Scientific, Alcobendas, Spain) was used to quantify isolated RNAs and 500 ng (cell culture) or 1 μg (tissue) samples of total RNAs were treated with DNase I (Life Technologies, Alcobendas, Spain), following the manufacturer's protocol, to remove all genomic DNA. Afterwards, total RNAs were reverse transcribed with the Transcriptor First Strand cDNA synthesis Kit (Roche, Sant Cugat del Valles, Spain). qRT-PCR was performed as previously described [39]. All the analyses were performed in triplicate using 384-well plates with 2.5 μL itaq SYBR Green Supermix (Bio-Rad, El Prat de Llobregat, Spain), 250 nM forward and reverse primers, and 1 μL cDNA for each sample, in a final volume of 5 μL. The primers were specific for acyl-CoA synthetase-1 (*acsl1*), beta-actin (*actb*), CCAAT/enhancer-binding protein alpha (*cebpa*), elongation factor 1 alpha (*ef1α*), fatty acid synthase (*fasn*), 3-hydroxyacyl-CoA dehydrogenase (*hoad*), hormone sensitive lipase (*lipe*), lipoprotein lipase (*lpl*), adipose triglyceride lipase (*pnpla2*), peroxisome proliferator activated receptor beta (*pparb*) and gamma (*pparg*), and *ubiquitin* (S1 Table).

Statistical analyses

Data were analyzed using IBM SPSS Statistics v.22 (IBM, Armonk, USA) and GraphPad prism 6 (La Jolla, USA, www.graphpad.com) and presented as mean ± SEM, unless stated otherwise. Normal distribution was first analyzed using the Shapiro-Wilk test, followed by Levene's to test homogeneity of variances. Statistical significance was assessed by two-tailed unpaired Student's t-test or one-way analysis of variance (ANOVA), followed by the Tukey *post-hoc* test. When data did not follow a normal distribution, a non-parametric Kruskal-Wallis test was applied, followed by a paired U-Mann Whitney test. Statistical differences were considered significant for all analyses when *p*-value $\leq$ 0.05, indicated by asterisks: $^*p \leq 0.05$, $^{**}p \leq 0.01$, $^{***}p \leq 0.0001$.

The mRNA level of each gene analyzed was calculated relative to the corresponding reference genes, i.e. geometric means of *ef1a* and *ubiquitin* for the *in vitro* cell culture assays and *ef1a* and *actb* for *in vivo* assays, using the Pfaffl method [40] implemented in the Biorad CFX manager 3.1 (Bio-Rad, El Prat de Llobregat, Spain).

Results

Identifying compounds of plant origin with antioxidant properties able to decrease zebrafish larval adiposity in vivo

To investigate the effect of CA, HT and ATX on the dynamics of zebrafish adiposity, ZOT was used as a non-invasive *in vivo* method for visualizing lipid droplets in living larvae by fluorescence microscopy [30]. The whole-body adiposity dynamics of each larva was expressed as a percentage of variation in Nile red fluorescence signal areas in fish previously fed on standard diet (SD) after one-day's exposure in a fasting state. The results revealed that exposure to 50 μM CA significantly decreased larval adiposity compared to CT-exposed fish (−22.83 ± 1.02% in CA *versus* −16.99 ± 1.29% with CT, $p \leq 0.01$) (Fig 1A). The same effect was observed with 100 μM HT (−29.72 ± 2.74% in HT *versus* −17.98 ± 1.97% with CT, $p \leq 0.05$)
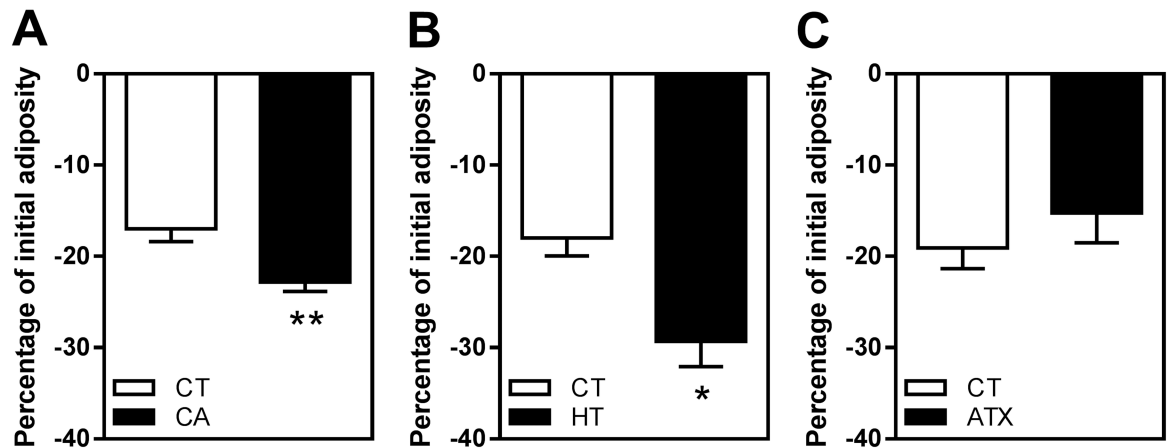
Fig 1. Identification of selected molecules of plant origin able to decrease adiposity *in vivo*. ZOT was conducted on larvae with a standard-length distribution from 7 to 9 mm and initially nourished with SD. Adiposity was quantified in fasting larvae in fish water with 0.1% DMSO as a vehicle control (CT) or 0.1% DMSO plus 50 μM CA (A), 100 μM HT (B), or 100 μM ATX (C). For each larva enrolled, WAT dynamics is expressed as a percentage of initial adiposity. Values are mean ± SEM, n = 4–6 independent experiments (10 animals per group). *$P \leq 0.05$, **$P \leq 0.01$ compared to CT, using two-tailed unpaired Student's t-test.

https://doi.org/10.1371/journal.pone.0178833.g001

(Fig 1B). In contrast, there was no change in adiposity following exposure to 100 μM ATX (Fig 1C).

Differential effect of CA and HT on WAT dynamics in different body parts

ZOT was used to study WAT dynamics in different body parts of zebrafish larvae, during exposure to the selected bioactive compounds. Perivisceral WAT accounted for around 60% of adiposity at these zebrafish larval developmental stages (S1 Fig). The remaining WAT in the head and tail regions represented around 30% and 10%, respectively (S1 Fig). Results showed that exposure to CA mainly affected adiposity in the head region, compared to the same region in CT fish (−10.85 ± 1.95% in CA *versus* −5.53 ± 0.54% with CT, $p \leq 0.05$) (Fig 2A). HT also led to a significant decrease in adiposity in the head (−11.46 ± 1.03% in HT *versus* −7.95 ± 0.24% with CT, $p \leq 0.05$) and viscera (−15.87 ± 2.23% in HT *versus* −7.13 ± 2.46% with CT, $p \leq 0.05$) compared to CT (Fig 2F). In contrast, ATX did not have a significant anti-obesogenic effect in any of the body regions (Fig 2K). Fluorescent images of isolated or grouped adipocytes revealed a marked decrease in oil droplet size following treatment with CA or HT (Fig 2C, 2E, 2H and 2J).

Potential antagonist effect of CA and HT on PPARγ signaling pathway

In view of the significant decrease in zebrafish larvae adiposity observed after treatment with CA and HT, the next step was to elucidate whether these compounds were capable of counter-acting the obesogenic effect of RGZ, a potential PPARγ agonist, *in vivo*. RGZ at 1 μM on an SD background diet was shown to prevent adiposity loss in fasting condition: −10.59 ± 1.35% in RGZ *versus* −18.1 ± 1.52% with CT, $p \leq 0.01$ (Fig 3A) and −14.23 ± 0.98% in RGZ *versus* −20.04 ± 0.88% with CT, $p \leq 0.05$ (Fig 3B). Simultaneous exposure of the larvae to RGZ and CA revealed that the obesogenic effect of RGZ was abolished by this compound (−−19.24 ± 0.40%) (Fig 3A). A similar effect was obtained following co-incubation with RGZ and HT (−23.47 ± 2.17%) (Fig 3B).
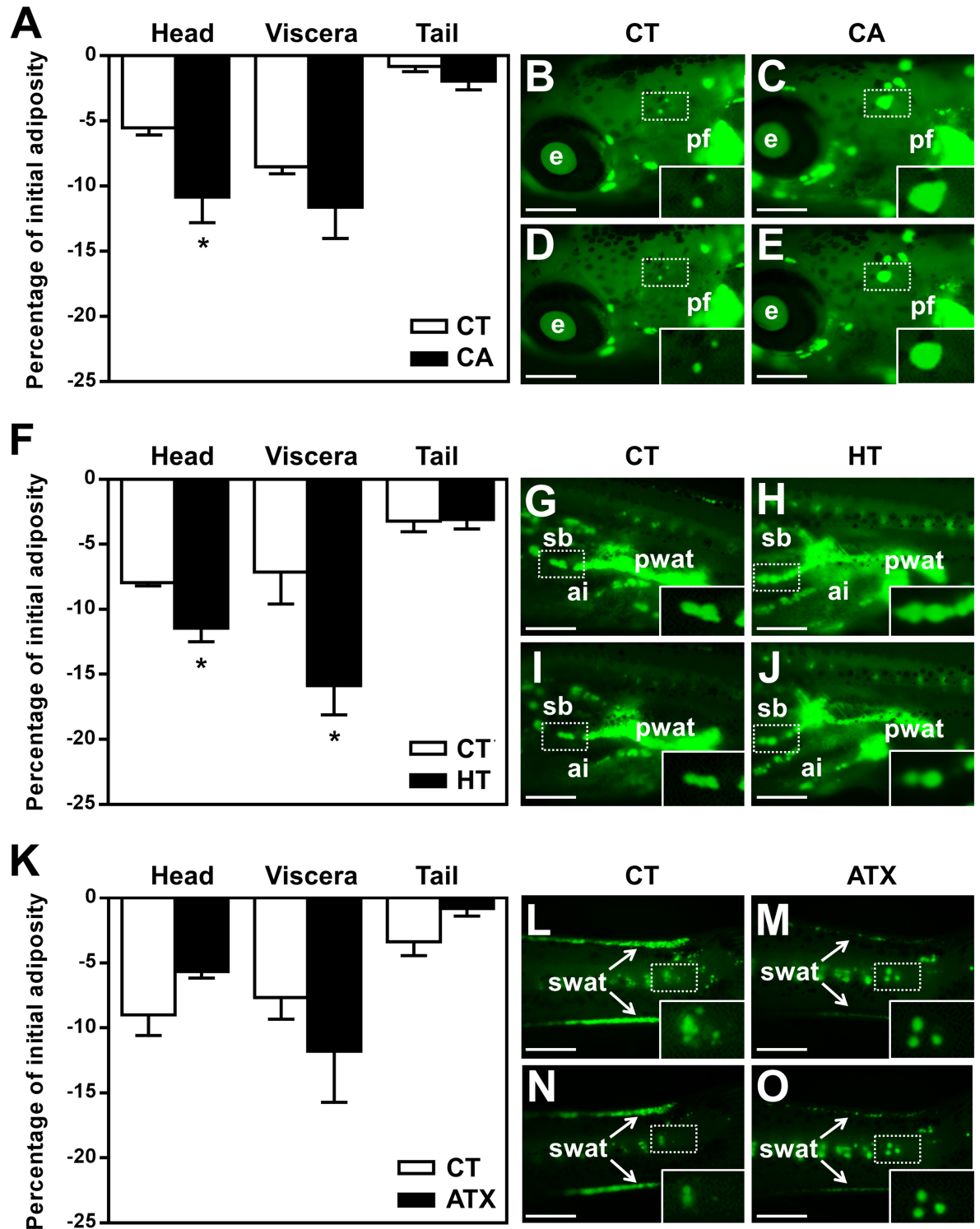
Fig 2. Differential effect of selected vegetal molecules of plant origin on WAT dynamics in different body parts of zebrafish larvae. Quantitative analysis of WAT dynamics was performed according to the ZOT protocol and the results are expressed as a percentage of initial adiposity relative to the amount of WAT fluorescence signal attached to each body region. Fasting larvae were exposed to 50 μM CA in 0.1% DMSO (A, C, E), 100 μM HT in 0.1% DMSO (F, H, J), 100 μM ATX in 0.1% DMSO (K, M, O), or 0.1% DMSO as a vehicle CT (A, B, D, F, G, I, K, L, N). Images of relevant regions in representative larvae are presented: head (B-E), viscera (G-J), and tail (L-O). Lateral views, anterior part on the left and dorsal part at the top, under fluorescence microscope after Nile red staining, recorded before (B, C, G, H, L, M) and after 24 h treatment (D, E, I, J, N, O) with

(CA, HT, ATX) or without (CT) exposure to the compounds. Insets in each image are enlarged views of isolated adipocytes or groups of adipocytes from each panel, marked by a white rectangle. Values are mean + SEM, n = 4–6 independent experiments (10 animals per group). *$p \leq 0.05$ compared to control for each region, using Student's t-test. Scale bar, 500 µm. Abbreviations: e, eye; pf, pectoral fin; pwat, perivisceral white adipose tissue; sb, swim bladder; ai, anterior intestine; swat, subcutaneous white adipose tissue.

https://doi.org/10.1371/journal.pone.0178833.g002
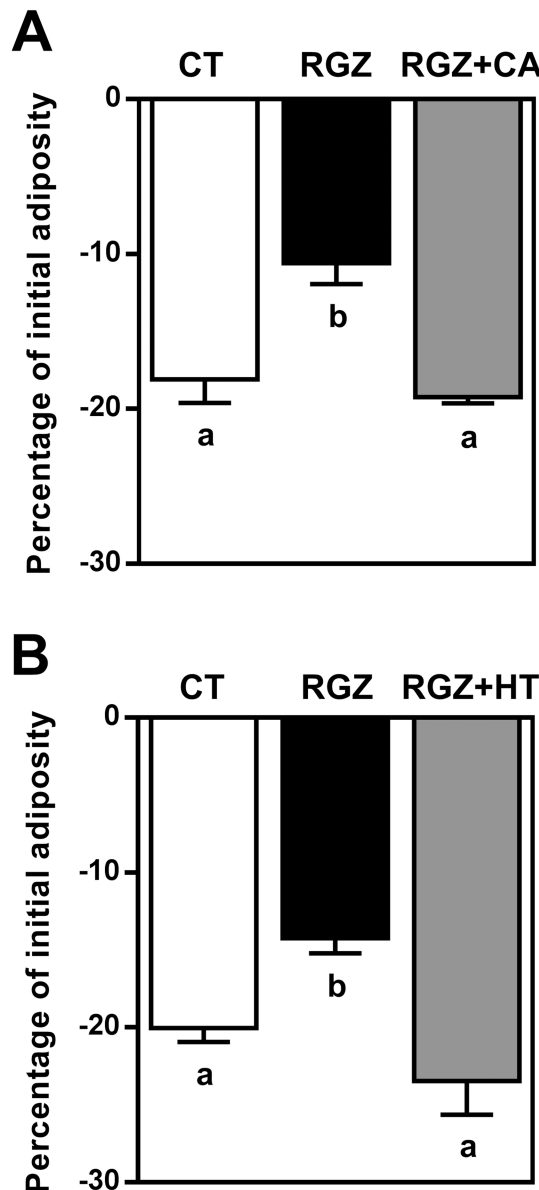
Fig 3. CA and HT abolished the *in vivo* obesogenic effect of RGZ. ZOT was applied to larvae previously nourished with SD. Adiposity was quantified in the presence of 0.1% DMSO as a vehicle CT or 0.1% DMSO plus the indicated combination of compounds. Exposure to 1 µM RGZ induced a significantly smaller decrease in adiposity compared with CT. The effect of RGZ was abolished by CA 50 µM (A) and HT (100 µM) (B). Values are mean ± SEM, n = 4 independent experiments (10 animals per group). Significant differences are shown as different letters ($p \leq 0.05$) using one-way ANOVA test followed by Tukey's *post hoc* test.

https://doi.org/10.1371/journal.pone.0178833.g003

Characterization of CA and HT effects on primary-cultured rainbow trout adipocytes

CA and HT significantly increased adipocyte viability (S2A Fig) without affecting proliferation (S2B Fig), whether the cells were co-treated with RGZ or not. RGZ alone or in combination with treatments did not affect cell viability or the percentage of PCNA-positive cells (S2 Fig). Quantification of the PPARγ immunofluorescence signal revealed that treating adipocytes with CA or HT in combination with RGZ significantly reduced the enhanced PPARγ protein expression signal produced by RGZ alone (Fig 4A and 4B). A very similar pattern although not showing significant differences was observed concerning PPARγ protein expression by Western blot (Fig 4C and 4D). A lower level of lipid storage was observed when these cells were cultured in the presence of lipid mixture (LIP)+CA and especially in the LIP+HT condition, compared to LIP alone (0.93 ± 0.176 and 0.56 ± 0.047 in LIP+CA and LIP+HT, respectively, *versus* 1.34 ± 0.13 with LIP, $p \leq 0.05$) (Fig 4E). Finally, qRT-PCR data revealed that LIP significantly increased the expression of *pparg* and *cebpa* transcripts compared to CT, whereas RGZ did not affect these values (Fig 4F and 4G). In addition, treatments with CA or HT slightly down-regulated *pparg* and *cebpa* mRNA levels when combined with LIP, whereas no changes were observed in combination with RGZ (Fig 4F and 4G).

In vivo effects of CA and HT on rainbow trout lipid metabolism

The next step was to clarify the role of CA and HT in an *in vivo* context by focusing on several key adipogenic, lipolitic and β-oxidation markers, as well as the potential cross talk between liver and WAT, using qRT-PCR and plasma parameters analyses. The data revealed that transcriptional levels of *fasn* in both WAT and liver were significantly decreased by HT treatment (Fig 5A and 5E), indicating a reduction in fatty acid synthesis, possibly resulting in a decrease in TAG formation and fat deposits. Moreover, *pnpla2* expression in WAT but not liver decreased significantly following HT administration (Fig 5D and 5H). On the other hand, *lipe1* mRNA levels in both liver and WAT were unaffected by CA or HT treatment (Fig 5C and 5G). Following CA administration, *lpl* mRNA levels were unaffected in WAT, but increased in liver, suggesting a higher TAG lipase activity in this tissue (Fig 5B and 5F). Regarding β-oxidation markers, *acsl1* mRNA levels presented a reverse regulation between tissues, being significantly increased by HT treatment in WAT and showing an opposite pattern but not significant in liver (Fig 6A and 6D). Aside from that, no changes were found in *hoad* (Fig 6B and 6E) nor *pparb* (Fig 6C and 6F) mRNA levels due to treatment in any tissue.

Since CA and HT were shown to modulate the expression of adipogenic, lipolytic and β-oxidation genes that regulate the lipid metabolism in both WAT and liver, it was useful to obtain further information by measuring blood parameters. Analysis of selected biochemical parameters in plasma revealed a slight decrease in TAG levels in fasting rainbow trout injected with CA and a significantly lower concentration with HT compared to CT (Table 1). However, no significant effects upon treatments were observed in plasma glucose nor NEFAs.

Discussion

While mammalian models have largely contributed to improving our understanding of obesity, in recent years, teleost models have also produced excellent findings on human diseases and offer a number of advantages [41]. Despite obvious differences, teleost fish share a significant amount of genetic identity with humans, and some metabolic pathways and organ systems are also remarkably similar [42,43]. Their rapid development ex-utero and the optical semi-transparency of the embryonic and early larval stages, as well as the advances in fish cell
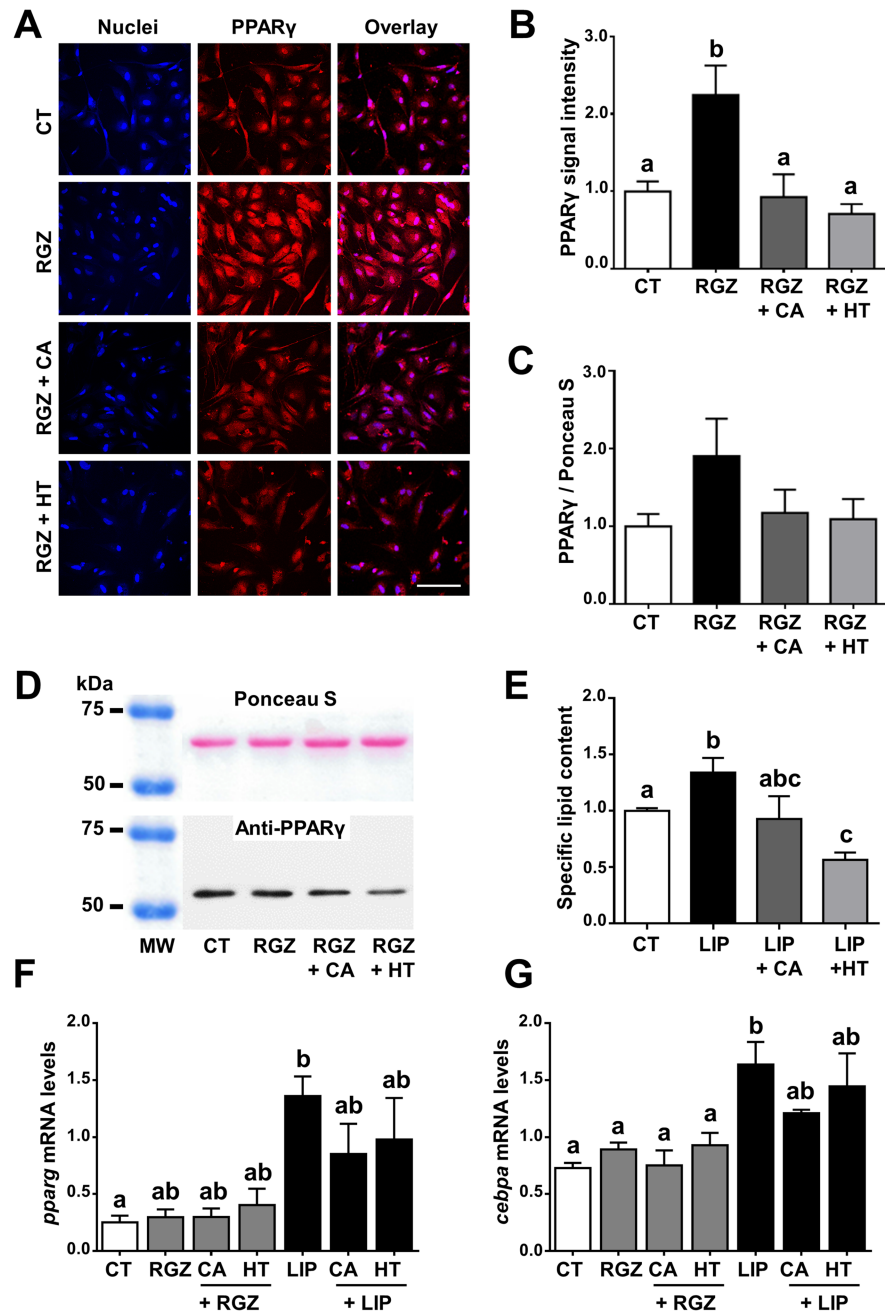
Fig 4. Characterization of potential PPARγ signaling pathway antagonism and inhibition of adipogenesis produced by CA and HT in primary-cultured rainbow trout adipocytes. Representative PPARγ immunofluorescence images (A), quantification of PPARγ immunofluorescence protein signal (B), anti-PPARγ immunoreactive band and quantification of PPARγ protein expression by Western blot (C, D), specific lipid content (E) and mRNA levels of adipogenic genes *pparg* (F) and *cebpa* (G). Immunofluorescence images show Hoechst nuclei staining (left panels), PPARγ (medium panels) and overlay (right panels). Scale bar, 100 µm. For both protein expression analyses (immunofluorescence, A and B; Western blot, C and D) cells were incubated with vehicle (DM) plus CA (50 µM), HT (100 µM), RGZ (1 µM), or the indicated combination of CA or HT with RGZ, or vehicle CT alone, for 24 h (day 7 of culture). RGZ was used as a potential rainbow trout PPARγ agonist. Representative Western blot images of anti-PPARγ immunoreactive band (top) and the same membrane labelled with Ponceau S (bottom) (D). Lipid content expressed spectrophotometrically as the ratio of absorbance value between ORO and Coomassie blue staining (E). For lipid content analysis cells were incubated with vehicle (DM) plus CA (50 µM), HT (100 µM), LIP (10 µl/ml), or the indicated combination of CA or HT with LIP, or vehicle CT alone, for 72 h (day 7 of

culture). mRNA levels of *pparg* (F) and *cebpa* (G) were normalized to the geometric mean of the two reference genes, *ef1a* and *ubiquitin*. For gene expression analyses cells were incubated with vehicle (DM) plus CA (50 µM), HT (100 µM), RGZ (1 µM), LIP (10 µl/ml), or the indicated combination of CA or HT with RGZ or LIP, or vehicle CT alone for 24 h (day 7 of culture). Data are shown as mean ± SEM (n = 3–7 cell cultures). Significant differences ($p \leq 0.05$) are indicated by different letters, using one-way ANOVA followed by Tukey's *post hoc* test (B, C, E, F) or the non-parametric Kruskal-Wallis test followed by paired U-Mann Whitney test (G).

https://doi.org/10.1371/journal.pone.0178833.g004

culture techniques have made teleost fish popular models in applied and basic research [14,21,41,42]. In mammals, fat deposits in specific regions differ from each other not only by localization but also by their structural and functional properties [44]. Similarly, WAT development in zebrafish is a step-wise process, with differentiated adipocytes first observed in the visceral region, then the subcutaneous area and finally, the head [27]. Moreover, zebrafish fat deposits are also mobilized sequentially, in reverse order, in response to starvation [20]; altogether highlighting the particular suitability of this species to study adiposity dynamics in an *in vivo* scenario.

Natural bioactive phytochemicals have recently attracted interest for their potential health benefits in preventing metabolic diseases, including obesity and insulin resistance [45]. Among these, dietary components of olive oil, red wine and marine algae are particularly interesting, due to their antioxidant properties, which are traditionally linked to longevity and reduced mortality from several diseases [46]. Furthermore, as well as obesogenic molecules, which predispose individuals to metabolic changes leading to weight gain [47], there is growing evidence that some plant compounds can improve overweight by inhibiting adipogenic
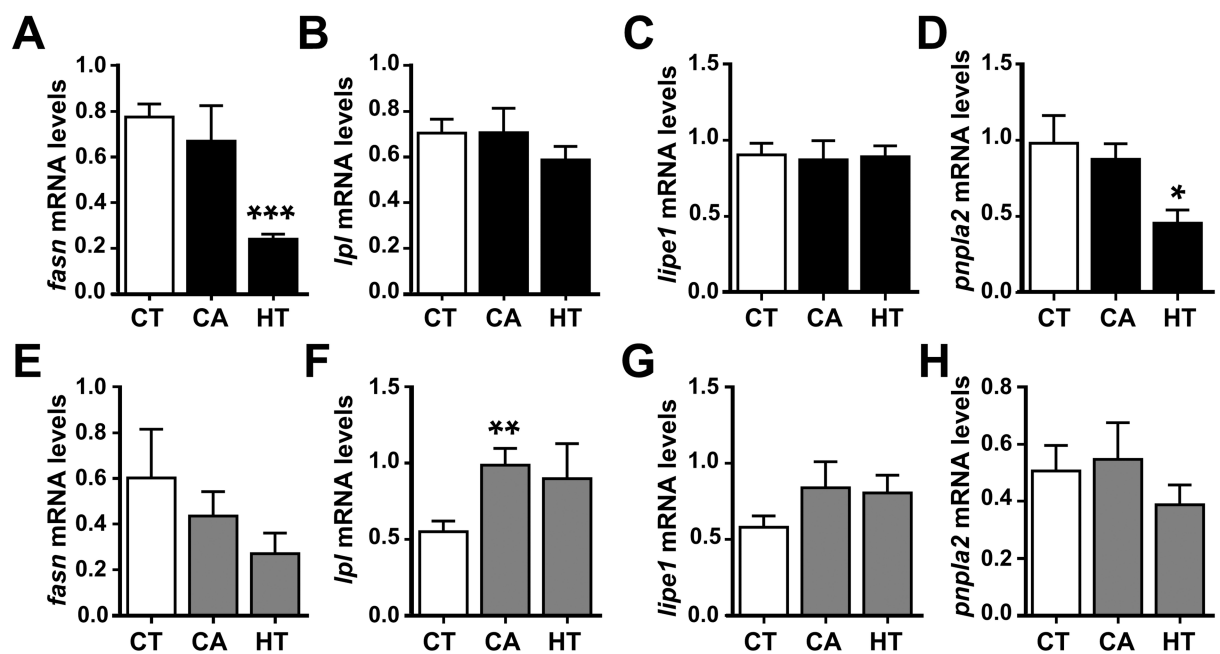
Fig 5. qRT-PCR analysis of selected lipid-metabolism-related gene transcript levels in the dissected periviceral WAT (A-D) and liver (E-H) of rainbow trout treated with CA and HT or untreated. After one-day fasting, juvenile rainbow trout received intraperitoneal injections of vehicle CT (DMSO in sesame oil 1:3, v/v), vehicle plus CA (10 µg/g body weight), or vehicle plus HT (20 µg/g body weight), and samples were taken after a 24 h exposure period in a fasting state. mRNA levels of *fasn* (A, E), *lpl* (B, F), *lipe1* (C, G) and *pnpla2* (D, H). All mRNA levels were normalized to the geometric mean of the two reference genes, *ef1a* and *actb*. Data are shown as mean ± SEM (n = 7–8 fish per condition). *$p \leq 0.05$, **$p \leq 0.01$, ***$p \leq 0.0001$, compared to CT, using Student's t-test.

https://doi.org/10.1371/journal.pone.0178833.g005
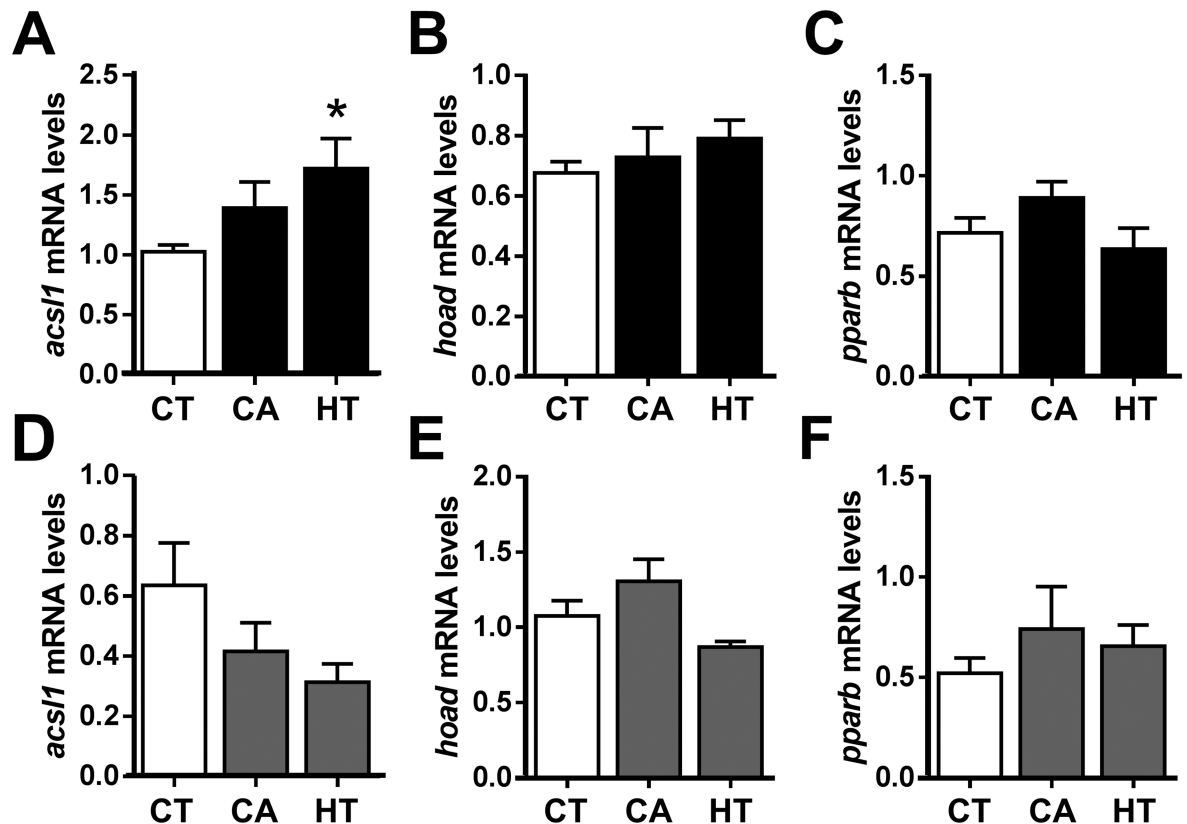
Fig 6. qRT-PCR analysis of selected β-oxidation-related gene transcript levels in the dissected perivisceral WAT (A-C) and liver (D-F) of rainbow trout treated with CA and HT or untreated. After one-day fasting, juvenile rainbow trout received intraperitoneal injections of vehicle CT (DMSO in sesame oil 1:3, v/v), vehicle plus CA (10 µg/g body weight), or vehicle plus HT (20 µg/g body weight), and samples were taken after a 24 h exposure period in a fasting state. mRNA levels of *acsl1* (A, D), *hoad* (B, E) and *pparb* (C, F). All mRNA levels were normalized to the geometric mean of the two reference genes, *ef1a* and *actb*. Data are shown as mean ± SEM (n = 7–8 fish per condition). *$p \leq 0.05$, compared to CT, using Student's t-test.

https://doi.org/10.1371/journal.pone.0178833.g006

pathways or impairing lipid accumulation and may, therefore, be classified as anti-obesogenic. Recent studies have reported that some phytochemicals and dietary supplements affect the lipid metabolism in zebrafish. Adding green tea extract to a high-fat diet significantly reduced body fat storage in adults [48,49]. Other studies of very early-stage larvae reported a decrease in lipids after treatment with compounds originating from plants or algae. The protocol

Table 1. Selected biochemical plasma parameters of rainbow trout intraperitoneally injected with CA or HT.

	CT	CA	HT
TAG (mmol/L)	4.69 ± 0.738	3.53 ± 0.164	2.59 ± 0.478*
Glycerol (DO 540 nm)	0.06 ± 0.0013	0.06 ± 0.0014	0.06 ± 0.0006
Glucose (mmol/L)	8.61 ± 1.077	6.86 ± 0.417	6.83 ± 0.480
NEFAs (mEq/L)	0.96 ± 0.074	1.02 ± 0.086	1.16 ± 0.133

Juvenile rainbow trout kept at 15°C received intraperitoneal injections after a one-day fast with vehicle CT, vehicle plus CA (10 µg/g), or vehicle plus HT (20 µg/g). After 24 h exposure to the compound, blood samples were harvested for further plasma biochemical analyses. The total fasting period was therefore 48 hours before blood sampling. Values are expressed as means ± SEM (n = 7 to 8 fish per condition). TAG, triacylglycerols; NEFAs, non-esterified fatty acids.

*$p < 0.05$ *versus* control using Student's t-test.

https://doi.org/10.1371/journal.pone.0178833.t001

consisted of a 15-day exposure to the compound on a high-fat diet background, starting at the first feeding period. For example, curcumin [50–53], indole-3-carbinol [54], baicalein [55], dieckol [56], ellagic acid [52], kaempferol [51], quercetin [56], seapolynol [57] and silibinin [58], have all been reported to inhibit lipid accumulation in these early, post-embryonic developmental stages, when the adipocyte lineage is just starting to be established [20,27]. In our work, we used the ZOT protocol at later larval developmental stages, when the animals had a well-established WAT [30]. *In vivo* Nile red staining of adipocyte lipid droplets and quantitative analysis of whole-mount wide-field fluorescence microscopy signals, before and after a one-day exposure to the selected chemical compounds, were used to monitor the dynamics of WAT mass linked to adipocyte droplet size rather than adipocyte cell number. In addition, this methodology discriminated between the lipid signals associated with WAT and liver and identified the potential modulation of different regional WAT fat deposits in zebrafish larvae.

In this context, the aim of the present study was to investigate the anti-obesogenic properties of three antioxidant compounds of plant origin, selected for their capacity to modulate the lipid metabolism in the 3T3-L1 adipocyte cell line and rodent models [59–64]. ATX is a natural red carotenoid pigment found in a wide variety of organisms, CA is one of the most abundant hydroxycinnamic acids in the human diet, and HT is bioavailable in olive leaves and olive oil. In the present work, CA and HT caused a significant, short-term reduction in zebrafish larval adiposity, but CA exhibited stronger anti-obesogenic effects only in the head region, initiating the reversal of the fat mobilization pattern, as described above, while HT affected both the head and visceral regions. These results indicate that these compounds reduce fat mass by decreasing adipocyte size, but they may have different anti-obesogenic capacities according to the WAT location in the body. As mentioned above, it is known that adipose deposits in different parts of the body have different biological functions and biochemical profiles. Several features, such as adipocyte growth and differentiation, developmental gene expression, susceptibility to apoptosis, inflammatory capacity, and adipokine secretion, vary among deposits, as well as fatty-acid processing and WAT enlargement and loss mechanisms [65]. Nevertheless, further investigation is required to determine how CA and HT target the specific needs of the different deposits. On the other hand, ATX did not modify the adiposity level of zebrafish, even when the different regions were analyzed separately. Although several studies support the hypothesis that ATX supplementation reduces body weight and fat accumulation in mice [66], the ATX action mechanism has been demonstrated to be cell-type dependent [62]. In agreement with our data, one study in humans reported that ATX did not boost fat utilization or fat loss [67].

Adipogenesis is a complex process that typically involves the sequential activation of several transcription factors, such as PPARγ, that regulate the differentiation of pre-adipocytes into mature adipocytes, and ultimately control WAT formation promoting both, lipogenesis and fatty acid uptake. In mammals, it has been demonstrated that CA and HT exhibit a significant potential to act as anti-obesity agents by modulating the PPARγ adipogenesis pathway [64,68]. Therefore, the potential antagonism of PPARγ produced by CA and HT may also disrupt fat accumulation in teleost fish and result in a reduction of WAT mass due to lipid storage impairment. Our results revealed that CA and HT abolished the RGZ-induced obesogenic effect in zebrafish. A similar inhibitory effect has been also reported in zebrafish exposed to specific pharmaceutical antagonists of RGZ [30,69], thus supporting the idea that the compounds used in the present study may antagonize PPARγ signaling.

During the last decade, *in vitro* cell culture models from fish species have been widely used for studies of lipid metabolism and adipocyte functionality [31,70,71]. Nevertheless, despite the increasing use of zebrafish as an obesity model, to our knowledge, a primary adipocyte cell culture from this species has not been developed up to date. In this regard, further

investigations using the well-established primary-cultured rainbow trout adipocyte system were performed in order to have a closer look into the potential PPARγ antagonism of CA and HT. The data supported the involvement of PPARγ in the mechanism underlying the anti-obesogenic activity of CA and HT. Concomitant with the counteracting effect downregulating the PPARγ protein expression signal induced by RGZ, CA and especially HT, also reduced the adipocyte lipid content, in agreement with our previous *in vivo* findings in zebrafish. However, qRT-PCR analyses revealed that these two compounds did not modulate the transcript levels of typical key markers of mature adipocytes, i.e. *pparg and cebpa*, when these cells were co-treated with RGZ, and had only a slight effect when they were combined with LIP. These findings suggest that the anti-obesogenic effect of CA and HT may be mediated by post-transcriptional mechanisms.

PPARγ deficiency and/or disruption directly not only affects WAT development and accumulation, but also exerts an impact on the whole body metabolism [72]. The *in vivo* administration experiment in rainbow trout revealed that CA and HT affected the mRNA levels of adipogenic and β-oxidation genes in liver and WAT in different ways. Fat loss is usually caused by the balance of two main processes: enhancement of fat breakdown and inhibition of TAG synthesis and accumulation. This process is orchestrated by the interaction of several tissues, such as WAT, liver and skeletal muscles [73]. The decrease in WAT *fasn* mRNA levels produced by HT treatment was accompanied by a reduction in plasma TAG levels, possibly due to the antagonist effect of this compound on the PPARγ signaling pathway. In agreement with our results, some mammal studies have demonstrated that CA and HT regulate WAT mass by suppressing lipogenic enzyme activity and claimed that PPARγ antagonists can be used to treat hyperlipidemia [74,75]. Interestingly, HT also downregulated *pnpla2* transcript abundance in rainbow trout WAT, which is indicative of decreased lipolysis, leading to a reduction in lipid turnover or compensation for excessive WAT decrease. On the other hand, CA administration increased *lpl* mRNA levels in the liver, also associated with the decreased TAG levels observed in plasma. Concomitant with this decrease, CA and HT also smoothly increased NEFAs levels via TAG hydrolysis. Moreover, a slight decrease was also observed in plasma glucose following treatment, in agreement with mammal studies where CA and HT have been proposed as potential hypoglycemic antidiabetic treatments [76,77]. Within this *in vivo* scenario it is important to notice that CA and HT are antioxidants, with proven effects upon cell viability (S2 Fig), which may have an implication in modulating fatty acid oxidation [78]. In this sense, HT administration upregulated *acsl1* mRNA levels in WAT while slightly decreased its expression in liver, indicating a tissue-specific regulation as previously reported [79]. Even though enhanced *acsl1* expression is traditionally believed to be essential for the synthesis of TAG, several studies in mammals revealed a possible function related to the β-oxidation of fatty acids [80,81], in agreement with our results. Nevertheless, differences were not observed concerning the mRNA levels of *hoad* and *pparb* suggesting that further studies are needed to better understand the potential involvement of CA and HT in WAT β-oxidation.

Conclusions

The findings reported here provide novel insights into the anti-obesogenic role of CA and HT antioxidants, highlighting their potential involvement in negatively modulating the PPARγ signaling pathway. Further studies using specific inhibitors of these nuclear receptors will help to understand the mechanism of action of these anti-obesogenic compounds. The teleost fish models used have been validated for studying the mode of action of these bioactive compounds on WAT, reinforcing their suitability in pharmacological and biomedical research. This study may also help the investigation of new additives to optimize adiposity in farmed animals.

Supporting information

S1 Fig. ZOT as a tool for studying WAT dynamics in different body parts of zebrafish larva. (A) External features of a representative 8 mm SL larva and images of head, viscera, and tail regions under a fluorescence microscope after Nile red staining, using HQ-FITC-BP filter, with adipocytes stained green. Lateral views, anterior part on the left and dorsal part at the top. (B) Quantitative analysis of adipocyte tissue area in each body region, expressed as a percentage of total adiposity. SL distribution of the animals used was from 7 to 9 mm. Boxplot shows median and percentile adiposity values, n = 11 independent experiments (10 animals per group). Scale bar: 0.5 mm. Abbreviations: ai, anterior intestine; cfa, caudal fin adipocytes; e, eye; pf, pectoral fin; pwat, perivisceral white adipose tissue; sb, swim bladder; swat, subcutaneous white adipose tissue.
(TIF)

S2 Fig. CA and HT increased cell viability but did not affect cell proliferation of rainbow trout adipocytes in primary culture. (A) Quantification of cell viability using MTT assay. (B) Cell proliferation determined by immunocytochemistry of PCNA. Cells were incubated with vehicle plus CA (50 μM), HT (100 μM), or RGZ (1 μM), alone or in combination, or vehicle CT alone, for 24 h (day 5 of culture). Data are shown as mean ± SEM (n = 3–4 cell cultures). $^{*}p \leq 0.05$, $^{**}p \leq 0.01$ compared to CT, using one-way ANOVA test followed by Tukey's *post hoc* test.
(TIF)

S1 Table. Nucleotide sequences of the primers used to evaluate mRNA abundance by qRT-PCR in rainbow trout.
(DOC)

Acknowledgments

Author Contributions

Conceptualization: EL PJB IN.

Data curation: EL PJB JG EC IN.

Formal analysis: EL PJB.

Funding acquisition: PJB JG EC IN.

Investigation: EL PJB EC.

Methodology: EL PJB EC.

Project administration: PJB IN.

Resources: PJB JG EC IN.

Software: EL PJB.

Supervision: PJB EC IN.

Validation: EL PJB IN.

Visualization: EL PJB.

Writing – original draft: EL PJB IN.

Writing – review & editing: EL PJB JG EC IN.

References

1. Pandita A, Sharma D, Pandita D, Pawar S, Tariq M, Kaul A. Childhood obesity: prevention is better than cure. Diabetes Metab Syndr Obes. 2016; 9: 83–9. https://doi.org/10.2147/DMSO.S90783 PMID: 27042133

2. Mitchell NS, Catenacci VA, Wyatt HR, Hill JO. Obesity: overview of an epidemic. Psychiatr Clin North Am. 2011; 34: 717–32. https://doi.org/10.1016/j.psc.2011.08.005 PMID: 22098799

3. Andrade-Oliveira V, Câmara NOS, Moraes-Vieira PM. Adipokines as drug targets in diabetes and underlying disturbances. J Diabetes Res. 2015; 2015: 681612. https://doi.org/10.1155/2015/681612 PMID: 25918733

4. Blüher M. Adipose tissue dysfunction contributes to obesity related metabolic diseases. Best Pract Res Clin Endocrinol Metab. Elsevier; 2013; 27: 163–77. https://doi.org/10.1016/j.beem.2013.02.005 PMID: 23731879

5. Lee J-E, Ge K. Transcriptional and epigenetic regulation of PPARγ expression during adipogenesis. Cell Biosci. BioMed Central; 2014; 4: 29. https://doi.org/10.1186/2045-3701-4-29 PMID: 24904744

6. Wang L, Waltenberger B, Pferschy-Wenzig E-M, Blunder M, Liu X, Malainer C, et al. Natural product agonists of peroxisome proliferator-activated receptor gamma (PPARγ): a review. Biochem Pharmacol. 2014; 92: 73–89. https://doi.org/10.1016/j.bcp.2014.07.018 PMID: 25083916

7. Grygiel-Górniak B. Peroxisome proliferator-activated receptors and their ligands: nutritional and clinical implications—a review. Nutr J. BioMed Central; 2014; 13: 17. https://doi.org/10.1186/1475-2891-13-17 PMID: 24524207

8. Hussein Z, Wentworth JM, Nankervis AJ, Proietto J, Colman PG. Effectiveness and side effects of thia-zolidinediones for type 2 diabetes: real-life experience from a tertiary hospital. Med J Aust. 2004; 181: 536–9. PMID: 15540964

9. Siraj FM, Natarajan S, Huq MA, Kim YJ, Yang DC. Structural investigation of ginsenoside Rf with PPARγ major transcriptional factor of adipogenesis and its impact on adipocyte. J Ginseng Res. 2015; 39: 141–7. https://doi.org/10.1016/j.jgr.2014.10.002 PMID: 26045687

10. Gülçin I. Antioxidant activity of caffeic acid (3,4-dihydroxycinnamic acid). Toxicology. 2006; 217: 213–20. https://doi.org/10.1016/j.tox.2005.09.011 PMID: 16243424

11. Gordon MH, Paiva-Martins F, Almeida M. Antioxidant activity of hydroxytyrosol acetate compared with that of other olive oil polyphenols. J Agric Food Chem. 2001; 49: 2480–5. PMID: 11368623

12. Naguib YM. Antioxidant activities of astaxanthin and related carotenoids. J Agric Food Chem. 2000; 48: 1150–4. PMID: 10775364

13. Lossi L, D'Angelo L, De Girolamo P, Merighi A. Anatomical features for an adequate choice of experimental animal model in biomedicine: II. Small laboratory rodents, rabbit, and pig. Ann Anat—Anat Anzeiger. 2016; 204: 11–28. https://doi.org/10.1016/j.aanat.2015.10.002 PMID: 26527557

14. D'Angelo L, Lossi L, Merighi A, de Girolamo P. Anatomical features for the adequate choice of experimental animal models in biomedicine: I. Fishes. Ann Anat—Anat Anzeiger. 2016; 205: 75–84. https://doi.org/10.1016/j.aanat.2016.02.001 PMID: 26925824

15. Song Y, Cone RD. Creation of a genetic model of obesity in a teleost. FASEB J. Federation of American Societies for Experimental Biology; 2007; 21: 2042–9. https://doi.org/10.1096/fj.06-7503com PMID: 17341684

16. Santoriello C, Zon LI. Hooked! Modeling human disease in zebrafish. J Clin Invest. American Society for Clinical Investigation; 2012; 122: 2337–43. https://doi.org/10.1172/JCI60434 PMID: 22751109

17. Caro M, Iturria I, Martinez-Santos M, Pardo MA, Rainieri S, Tueros I, et al. Zebrafish dives into food research: effectiveness assessment of bioactive compounds. Food Funct. 2016; 7: 2615–23. https://doi.org/10.1039/c6fo00046k PMID: 27109696

18. Yada T, Moriyama S, Suzuki Y, Azuma T, Takahashi A, Hirose S, et al. Relationships between obesity and metabolic hormones in the "cobalt" variant of rainbow trout. Gen Comp Endocrinol. 2002; 128: 36–43. https://doi.org/10.1016/S0016-6480(02)00047-3 PMID: 12270786

19. Albalat A, Saera-Vila A, Capilla E, Gutiérrez J, Pérez-Sánchez J, Navarro I. Insulin regulation of lipopro-tein lipase (LPL) activity and expression in gilthead sea bream (*Sparus aurata*). Comp Biochem Physiol Part B Biochem Mol Biol. 2007; 148: 151–159. https://doi.org/10.1016/j.cbpb.2007.05.004 PMID: 17600746

20. Flynn EJ, Trent CM, Rawls JF. Ontogeny and nutritional control of adipogenesis in zebrafish (*Danio rerio*). J Lipid Res. 2009; 50: 1641–52. https://doi.org/10.1194/jlr.M800590-JLR200 PMID: 19366995

21. Bou M, Todorčević M, Torgersen J, Škugor S, Navarro I, Ruyter B. De novo lipogenesis in Atlantic salmon adipocytes. Biochim Biophys Acta—Gen Subj. 2016; 1860: 86–96. https://doi.org/10.1016/j.bbagen.2015.10.022 PMID: 26518346

22. Pignatelli J, Castro R, González Granja A, Abós B, González L, Jensen LB, et al. Immunological charac-terization of the teleost adipose tissue and its modulation in response to viral infection and fat-content in the diet. Trottein F, editor. PLoS One. 2014; 9: e110920. https://doi.org/10.1371/journal.pone.0110920 PMID: 25333488

23. Johansson M, Morgenroth D, Einarsdottir IE, Gong N, Björnsson BT. Energy stores, lipid mobilization and leptin endocrinology of rainbow trout. J Comp Physiol B. 2016; 186: 759–773. https://doi.org/10.1007/s00360-016-0988-y PMID: 27083432

24. Babin PJ, Vernier JM. Plasma lipoproteins in fish. J Lipid Res. 1989; 30: 467–89. PMID: 2666541

25. Babin PJ, Gibbons GF. The evolution of plasma cholesterol: direct utility or a "spandrel"; of hepatic lipid metabolism? Prog Lipid Res. 2009; 48: 73–91. https://doi.org/10.1016/j.plipres.2008.11.002 PMID: 19049814

26. Den Broeder MJ, Kopylova VA, Kamminga LM, Legler J. Zebrafish as a model to study the role of perox-isome proliferating-activated receptors in adipogenesis and obesity. PPAR Res. 2015; 2015: 358029. https://doi.org/10.1155/2015/358029 PMID: 26697060

27. Imrie D, Sadler KC. White adipose tissue development in zebrafish is regulated by both developmental time and fish size. Dev Dyn. 2010; 239: 3013–23. https://doi.org/10.1002/dvdy.22443 PMID: 20925116

28. McMenamin SK, Minchin JEN, Gordon TN, Rawls JF, Parichy DM. Dwarfism and increased adiposity in the gh1 mutant zebrafish vizzini. Endocrinology. The Endocrine Society; 2013; 154: 1476–87. https://doi.org/10.1210/en.2012-1734 PMID: 23456361

29. Minchin JEN, Dahlman I, Harvey CJ, Mejhert N, Singh MK, Epstein JA, et al. Plexin D1 determines body fat distribution by regulating the type V collagen microenvironment in visceral adipose tissue. Proc Natl Acad Sci U S A. National Academy of Sciences; 2015; 112: 4363–8. https://doi.org/10.1073/pnas.1416412112 PMID: 25831505

30. Tingaud-Sequeira A, Ouadah N, Babin PJ. Zebrafish obesogenic test: a tool for screening molecules that target adiposity. J Lipid Res. 2011; 52: 1765–72. https://doi.org/10.1194/jlr.D017012 PMID: 21724975

31. Bouraoui L, Gutiérrez J, Navarro I. Regulation of proliferation and differentiation of adipocyte precursor cells in rainbow trout (*Oncorhynchus mykiss*). J Endocrinol. 2008; 198: 459–69. https://doi.org/10.1677/JOE-08-0264 PMID: 18579724

32. Vélez EJ, Lutfi E, Jiménez-Amilburu V, Riera-Codina M, Capilla E, Navarro I, et al. IGF-I and amino acids effects through TOR signaling on proliferation and differentiation of gilthead sea bream cultured myocytes. Gen Comp Endocrinol. 2014; 205: 296–304. https://doi.org/10.1016/j.ygcen.2014.05.024 PMID: 24882593

33. Bradford MM. A rapid and sensitive method for the quantitation of microgram quantities of protein utiliz-ing the principle of protein-dye binding. Anal Biochem. 1976; 72: 248–254. PMID: 942051

34. Bou M, Todorčević M, Rodríguez J, Capilla E, Gutiérrez J, Navarro I. Interplay of adiponectin, TNFα and insulin on gene expression, glucose uptake and PPARγ, AKT and TOR pathways in rainbow trout cultured adipocytes. Gen Comp Endocrinol. 2014; 205: 218–225. https://doi.org/10.1016/j.ygcen.2014.05.005 PMID: 24846393

35. Olesen KM, Auger AP. Sex differences in fos protein expression in the neonatal rat brain. J Neuroendo-crinol. Blackwell Science Ltd; 2005; 17: 255–261. https://doi.org/10.1111/j.1365-2826.2005.01302.x PMID: 15842237

36. Romero-Calvo I, Ocón B, Martínez-Moya P, Suárez MD, Zarzuelo A, Martínez-Augustin O, et al. Reversible Ponceau staining as a loading control alternative to actin in Western blots. Anal Biochem. 2010; 401: 318–320. https://doi.org/10.1016/j.ab.2010.02.036 PMID: 20206115

37. Vélez EJ, Azizi S, Lutfi E, Capilla E, Moya A, Navarro I, et al. Moderate and sustained exercise modu-lates muscle proteolytic and myogenic markers in gilthead sea bream (*Sparus aurata*). Am J Physiol—Regul Integr Comp Physiol. 2017; ajpregu.00308.2016. https://doi.org/10.1152/ajpregu.00308.2016 PMID: 28228414

38. Capilla E, Teles-García A, Acerete L, Navarro I, Gutiérrez J. Insulin and IGF-I effects on the proliferation of an osteoblast primary culture from sea bream (*Sparus aurata*). Gen Comp Endocrinol. 2011; 172: 107–14. https://doi.org/10.1016/j.ygcen.2011.03.020 PMID: 21447336

39. Salmerón C, García de la serrana D, Jiménez-Amilburu V, Fontanillas R, Navarro I, Johnston IA, et al. Characterisation and expression of calpain family members in relation to nutritional status, diet composition and flesh texture in gilthead sea bream (*Sparus aurata*). PLoS One. 2013; 8: e75349. https://doi.org/10.1371/journal.pone.0075349 PMID: 24086513

40. Pfaffl MW. A new mathematical model for relative quantification in real-time RT-PCR. Nucleic Acids Res. 2001; 29: e45. PMID: 11328886

41. Santoro MM. Zebrafish as a model to explore cell metabolism. Trends Endocrinol Metab. Elsevier; 2014; 25: 546–54. https://doi.org/10.1016/j.tem.2014.06.003 PMID: 24997878

42. Seth A, Stemple DL, Barroso I. The emerging use of zebrafish to model metabolic disease. Dis Model Mech. 2013; 6: 1080–8. https://doi.org/10.1242/dmm.011346 PMID: 24046387

43. Oka T, Nishimura Y, Zang L, Hirano M, Shimada Y, Wang Z, et al. Diet-induced obesity in zebrafish shares common pathophysiological pathways with mammalian obesity. BMC Physiol. 2010; 10: 21. https://doi.org/10.1186/1472-6793-10-21 PMID: 20961460

44. Bjørndal B, Burri L, Staalesen V, Skorve J, Berge RK, Berge RK. Different adipose depots: their role in the development of metabolic syndrome and mitochondrial response to hypolipidemic agents. J Obes. Hindawi Publishing Corporation; 2011; 2011: 490650. https://doi.org/10.1155/2011/490650 PMID: 21403826

45. Huang C-C, Tung Y-T, Huang W-C, Chen Y-M, Hsu Y-J, Hsu M-C. Beneficial effects of cocoa, coffee, green tea, and garcinia complex supplement on diet induced obesity in rats. BMC Complement Altern Med. 2016; 16: 100. https://doi.org/10.1186/s12906-016-1077-1 PMID: 26968378

46. Sadowska-Bartosz I, Bartosz G. Effect of antioxidants supplementation on aging and longevity. Biomed Res Int. 2014; 2014: 404680. https://doi.org/10.1155/2014/404680 PMID: 24783202

47. Grün F, Blumberg B. Environmental obesogens: organotins and endocrine disruption via nuclear receptor signaling. Endocrinology. Endocrine Society; 2006; 147: s50–s55. https://doi.org/10.1210/en.2005-1129 PMID: 16690801

48. Hasumura T, Shimada Y, Kuroyanagi J, Nishimura Y, Meguro S, Takema Y, et al. Green tea extract suppresses adiposity and affects the expression of lipid metabolism genes in diet-induced obese zebrafish. Nutr Metab (Lond). 2012; 9: 73. https://doi.org/10.1186/1743-7075-9-73 PMID: 22871059

49. Meguro S, Hasumura T, Hase T. Body fat accumulation in zebrafish is induced by a diet rich in fat and reduced by supplementation with green tea extract. PLoS One. 2015; 10: e0120142. https://doi.org/10.1371/journal.pone.0120142 PMID: 25785691

50. Choi H-S, Jeon H-J, Lee O-H, Lee B-Y. Dieckol, a major phlorotannin in Ecklonia cava, suppresses lipid accumulation in the adipocytes of high-fat diet-fed zebrafish and mice: Inhibition of early adipogenesis via cell-cycle arrest and AMPKα activation. Mol Nutr Food Res. 2015; 59: 1458–71. https://doi.org/10.1002/mnfr.201500021 PMID: 25944759

51. Lee Y-J, Choi H-S, Seo M-J, Jeon H-J, Kim K-J, Lee B-Y. Kaempferol suppresses lipid accumulation by inhibiting early adipogenesis in 3T3-L1 cells and zebrafish. Food Funct. 2015; 6: 2824–33. https://doi.org/10.1039/c5fo00481k PMID: 26174858

52. Woo M-S, Choi H-S, Seo M-J, Jeon H-J, Lee B-Y. Ellagic acid suppresses lipid accumulation by suppressing early adipogenic events and cell cycle arrest. Phytother Res. 2015; 29: 398–406. https://doi.org/10.1002/ptr.5264 PMID: 25462071

53. Kim JH, Kang S, Jung YN, Choi H-S. Cholecalciferol inhibits lipid accumulation by regulating early adipogenesis in cultured adipocytes and zebrafish. Biochem Biophys Res Commun. 2016; 469: 646–53. https://doi.org/10.1016/j.bbrc.2015.12.049 PMID: 26703207

54. Choi H-S, Jeon H-J, Lee O-H, Lee B-Y. Indole-3-carbinol, a vegetable phytochemical, inhibits adipogenesis by regulating cell cycle and AMPKα signaling. Biochimie. 2014; 104: 127–36. https://doi.org/10.1016/j.biochi.2014.06.010 PMID: 24952351

55. Seo M-J, Choi H-S, Jeon H-J, Woo M-S, Lee B-Y. Baicalein inhibits lipid accumulation by regulating early adipogenesis and m-TOR signaling. Food Chem Toxicol. 2014; 67: 57–64. https://doi.org/10.1016/j.fct.2014.02.009 PMID: 24560969

56. Seo M-J, Lee Y-J, Hwang J-H, Kim K-J, Lee B-Y. The inhibitory effects of quercetin on obesity and obesity-induced inflammation by regulation of MAPK signaling. J Nutr Biochem. 2015; 26: 1308–16. https://doi.org/10.1016/j.jnutbio.2015.06.005 PMID: 26277481

57. Jeon H-J, Choi H-S, Lee Y-J, Hwang J-H, Lee O-H, Seo M-J, et al. Seapolynol extracted from ecklonia cava inhibits adipocyte differentiation *in vitro* and decreases fat accumulation *in vivo*. Molecules. 2015; 20: 21715–31. https://doi.org/10.3390/molecules201219796 PMID: 26690099

58. Suh HJ, Cho SY, Kim EY, Choi H-S. Blockade of lipid accumulation by silibinin in adipocytes and zebra-fish. Chem Biol Interact. 2015; 227: 53–62. https://doi.org/10.1016/j.cbi.2014.12.027 PMID: 25559859

59. Ikeuchi M, Koyama T, Takahashi J, Yazawa K. Effects of astaxanthin in obese mice fed a high-fat diet. Biosci Biotechnol Biochem. 2007; 71: 893–9. https://doi.org/10.1271/bbb.60521 PMID: 17420580

60. Cho A-S, Jeon S-M, Kim M-J, Yeo J, Seo K-I, Choi M-S, et al. Chlorogenic acid exhibits anti-obesity property and improves lipid metabolism in high-fat diet-induced-obese mice. Food Chem Toxicol. 2010; 48: 937–43. https://doi.org/10.1016/j.fct.2010.01.003 PMID: 20064576

61. Drira R, Chen S, Sakamoto K. Oleuropein and hydroxytyrosol inhibit adipocyte differentiation in 3 T3-L1 cells. Life Sci. 2011; 89: 708–16. https://doi.org/10.1016/j.lfs.2011.08.012 PMID: 21945192

62. Inoue M, Tanabe H, Matsumoto A, Takagi M, Umegaki K, Amagaya S, et al. Astaxanthin functions differently as a selective peroxisome proliferator-activated receptor γ modulator in adipocytes and macrophages. Biochem Pharmacol. Elsevier Inc.; 2012; 84: 692–700. https://doi.org/10.1016/j.bcp.2012.05.021 PMID: 22732454

63. Drira R, Sakamoto K. Modulation of adipogenesis, lipolysis and glucose consumption in 3T3-L1 adipocytes and C2C12 myotubes by hydroxytyrosol acetate: a comparative study. Biochem Biophys Res Commun. 2013; 440: 576–81. https://doi.org/10.1016/j.bbrc.2013.09.106 PMID: 24099771

64. Drira R, Sakamoto K. Hydroxytyrosol stimulates lipolysis via A-kinase and extracellular signal-regulated kinase activation in 3T3-L1 adipocytes. Eur J Nutr. 2014; 53: 743–50. https://doi.org/10.1007/s00394-013-0578-7 PMID: 23995352

65. Tchkonia T, Thomou T, Zhu Y, Karagiannides I, Pothoulakis C, Jensen MD, et al. Mechanisms and metabolic implications of regional differences among fat depots. Cell Metab. 2013; 17: 644–56. https://doi.org/10.1016/j.cmet.2013.03.008 PMID: 23583168

66. Arunkumar E, Bhuvaneswari S, Anuradha CV. An intervention study in obese mice with astaxanthin, a marine carotenoid—effects on insulin signaling and pro-inflammatory cytokines. Food Funct. The Royal Society of Chemistry; 2012; 3: 120–6. https://doi.org/10.1039/c1fo10161g PMID: 22089895

67. Res PT, Cermak NM, Stinkens R, Tollakson TJ, Haenen GR, Bast A, et al. Astaxanthin supplementation does not augment fat use or improve endurance performance. Med Sci Sports Exerc. 2013; 45: 1158–65. https://doi.org/10.1249/MSS.0b013e31827fddc4 PMID: 23274592

68. Liao C, Ou T, Wu C, Wang C. Prevention of diet-induced hyperlipidemia and obesity by caffeic acid in C57BL/6 mice through regulation of hepatic lipogenesis gene expression. J Agric Food Chem. 2013; 61: 11082–11088. https://doi.org/10.1021/jf4026647 PMID: 24156384

69. Ouadah-Boussouf N, Babin PJ. Pharmacological evaluation of the mechanisms involved in increased adiposity in zebrafish triggered by the environmental contaminant tributyltin. Toxicol Appl Pharmacol. 2016; 294: 32–42. https://doi.org/10.1016/j.taap.2016.01.014 PMID: 26812627

70. Vegusdal A, Sundvold H, Gjøen T, Ruyter B. An in vitro method for studying the proliferation and differentiation of Atlantic salmon preadipocytes. Lipids. 2003; 38: 289–96. PMID: 12784870

71. Salmerón C, Johansson M, Asaad M, Angotzi AR, Rønnestad I, Stefansson SO, et al. Roles of leptin and ghrelin in adipogenesis and lipid metabolism of rainbow trout adipocytes in vitro. Comp Biochem Physiol -Part A Mol Integr Physiol. 2015; 188: 40–48. https://doi.org/10.1016/j.cbpa.2015.06.017 PMID: 26103556

72. Celi FS, Shuldiner AR. The role of peroxisome proliferator-activated receptor gamma in diabetes and obesity. Curr Diab Rep. 2002; 2: 179–185. https://doi.org/10.1007/s11892-002-0078-2 PMID: 12643137

73. Samdani P, Singhal M, Sinha N, Tripathi P, Sharma S, Tikoo K, et al. A Comprehensive inter-tissue crosstalk analysis underlying progression and control of obesity and diabetes. Sci Rep. Nature Publishing Group; 2015; 5: 12340. https://doi.org/10.1038/srep12340 PMID: 26202695

74. Vanella L, Tibullo D, Godos J, Pluchinotta FR, Di Giacomo C, Sorrenti V, et al. Caffeic acid phenethyl ester regulates PPAR's levels in stem cells-derived adipocytes. PPAR Res. 2016; 2016: 7359521. https://doi.org/10.1155/2016/7359521 PMID: 26904104

75. Tutino V, Orlando A, Russo F, Notarnicola M. Hydroxytyrosol inhibits cannabinoid CB1 receptor gene expression in 3T3-L1 preadipocyte cell line. J Cell Physiol. 2016; 231: 483–9. https://doi.org/10.1002/jcp.25094 PMID: 26189725

76. Jung UJ, Lee M-K, Park YB, Jeon S-M, Choi M-S. Antihyperglycemic and antioxidant properties of caffeic acid in db/db mice. J Pharmacol Exp Ther. 2006; 318: 476–83. https://doi.org/10.1124/jpet.106.105163 PMID: 16644902

77. Jemai H, El Feki A, Sayadi S. Antidiabetic and antioxidant effects of hydroxytyrosol and oleuropein from olive leaves in alloxan-diabetic rats. J Agric Food Chem. 2009; 57: 8798–804. https://doi.org/10.1021/jf901280r PMID: 19725535

78. Gutierrez VR, de la Puerta R, Catalá A. The effect of tyrosol, hydroxytyrosol and oleuropein on the non-enzymatic lipid peroxidation of rat liver microsomes. Mol Cell Biochem. 2001; 217: 35–41. PMID: 11269663

79. Mashek DG, Li LO, Coleman RA. Long-chain acyl-CoA synthetases and fatty acid channeling. Future Lipidol. NIH Public Access; 2007; 2: 465–476. https://doi.org/10.2217/17460875.2.4.465 PMID: 20354580

80. Li LO, Ellis JM, Paich HA, Wang S, Gong N, Altshuller G, et al. Liver-specific loss of long chain acyl-CoA synthetase-1 decreases triacylglycerol synthesis and beta-oxidation and alters phospholipid fatty acid composition. J Biol Chem. American Society for Biochemistry and Molecular Biology; 2009; 284: 27816–26. https://doi.org/10.1074/jbc.M109.022467 PMID: 19648649

81. Ellis JM, Li LO, Wu P-C, Koves TR, Ilkayeva O, Stevens RD, et al. Adipose acyl-CoA synthetase-1 directs fatty acids toward beta-oxidation and is required for cold thermogenesis. Cell Metab. NIH Public Access; 2010; 12: 53–64. https://doi.org/10.1016/j.cmet.2010.05.012 PMID: 20620995